

Diverse impacts of the Indian summer monsoon on ENSO among CMIP6 models and its possible causes

Article

Published Version

Creative Commons: Attribution 4.0 (CC-BY)

Open Access

Lin, S., Dong, B. ORCID: https://orcid.org/0000-0003-0809-7911, Yang, S. and Zhang, T. (2024) Diverse impacts of the Indian summer monsoon on ENSO among CMIP6 models and its possible causes. Environmental Research Letters, 19 (8). 084052. ISSN 1748-9326 doi: 10.1088/1748-9326/ad6618 Available at https://centaur.reading.ac.uk/117423/

It is advisable to refer to the publisher's version if you intend to cite from the work. See Guidance on citing.

To link to this article DOI: http://dx.doi.org/10.1088/1748-9326/ad6618

Publisher: Institute of Physics

All outputs in CentAUR are protected by Intellectual Property Rights law, including copyright law. Copyright and IPR is retained by the creators or other copyright holders. Terms and conditions for use of this material are defined in the End User Agreement.

www.reading.ac.uk/centaur



CentAUR

Central Archive at the University of Reading Reading's research outputs online



LETTER • OPEN ACCESS

Diverse impacts of the Indian summer monsoon on ENSO among CMIP6 models and its possible causes

To cite this article: Shuheng Lin et al 2024 Environ. Res. Lett. 19 084052

View the article online for updates and enhancements.

You may also like

- Reduction of mid-summer rainfall in northern India after the late-1990s induced by the decadal change of the Silk Road pattern Xi Wang, Riyu Lu and Xiaowei Hong
- Shift in Indian summer monsoon onset A S Sahana, Subimal Ghosh, Auroop
- Ganguly et al. - Dynamical influence of MJO phases on the
- onset of Indian monsoon S Lenka, Krushna Chandra Gouda, Rani Devi et al.



ENVIRONMENTAL RESEARCH

LETTERS



OPEN ACCESS

RECEIVED

18 January 2024

REVISED

5 June 2024

ACCEPTED FOR PUBLICATION 22 July 2024

PUBLISHED

2 August 2024

Original content from this work may be used under the terms of the Creative Commons Attribution 4.0 licence.

Any further distribution of this work must maintain attribution to the author(s) and the title of the work, journal citation and DOI.



LETTER

Diverse impacts of the Indian summer monsoon on ENSO among CMIP6 models and its possible causes

Shuheng Lin^{1,2}, Buwen Dong³, Song Yang^{2,4,*} and Tuantuan Zhang^{2,4}

- ¹ Key Laboratory of Humid Subtropical Eco-geographical Process (Ministry of Education), College of Geographical Sciences, Fujian Normal University, Fuzhou, People's Republic of China
- ² School of Atmospheric Sciences, Sun Yat-sen University; Southern Marine Science and Engineering Guangdong Laboratory (Zhuhai), Zhuhai, People's Republic of China
- ³ National Centre for Atmospheric Science, Department of Meteorology, University of Reading, Reading, United Kingdom
- ⁴ Guangdong Province Key Laboratory for Climate Change and Natural Disaster Studies, Sun Yat-sen University, Zhuhai, People's Republic of China
- * Author to whom any correspondence should be addressed.

E-mail: yangsong3@mail.sysu.edu.cn

Keywords: Indian summer monsoon, ENSO, CMIP6, air-sea interactions, climate models

Supplementary material for this article is available online

Abstract

This study examines the performance of 52 models from phase 6 of the Coupled Model Intercomparison Project (CMIP6) in capturing the effects of the Indian summer monsoon on the evolution of El Niño–Southern Oscillation (ENSO). The ISM's impacts on ENSO show a substantial diversity among the models. While some models simulate the strength of the impacts comparable to observations, others represent much weaker influences. Results indicate that the diversity is highly related to inter-model spread in interannual variability of ISM rainfall (ISMR) among the models. Models with a larger ISMR variability simulate stronger ISM-induced anomalies in precipitation and atmospheric circulation over the western North Pacific during the monsoon season. As a result, these models exhibit larger wind anomalies induced by monsoon on the south flank of the anomalous circulation in the western Pacific, thereby influencing subsequent ENSO evolution more significantly by causing stronger air-sea coupling processes over the tropical Pacific.

1. Introduction

The Indian summer monsoon (ISM), or South Asian summer monsoon, is an important component of the Asian monsoon system. It exerts pronounced impacts on the ecosystem and human activities in densely populated regions (Gadgil and Gadgil 2006, Wahl and Morrill 2010, Chowdary et al 2021). The El Niño-Southern Oscillation (ENSO), originating in the tropical Pacific, is a major driver of global climate variability on interannual timescale (Zhang et al 1999, Yeh et al 2018, Yang et al 2018b, Taschetto et al 2020). The relationships between these two vital climate systems have long been a focal topic in climate research. It has been well known that during the developing summer of El Niño (La Niña), the ISM rainfall (ISMR) tends to be weaker (stronger) than normal, with a negative simultaneous correlation between the two (Rasmusson and Carpenter 1983, Webster

and Yang 1992, Miyakoda et al 2003, Kumar et al 2006). The impacts of ENSO on ISM are primarily established through the ENSO-induced anomalous Walker circulation during the monsoon season (June-September, JJAS) (Pant and Parthasarathy 1981, Ju and Slingo 1995, Kumar et al 1999, 2006). On the other hand, previous studies have proposed that the ISM could also influence ENSO. Both ENSO and the monsoon are integral components of the coupled climate system, and they interact with each other (Webster and Yang 1992, Yang et al 2018a, Yuan et al 2020). The lead-lag relationship between ISMR and sea surface temperature (SST) anomalies in the central-eastern Pacific features as a maximum negative correlation when the SST anomalies (SSTAs) lag the ISMR by 3-6 months (Yasunari 1990, Lau and Yang 1996, Kirtman and Shukla 2000). In addition, composite analyses based on anomalous ISM years show that when the ISM is stronger (weaker)

than normal, the Pacific trade winds become stronger (weaker) than average, accompanied by cold (warm) SSTAs in the eastern Pacific (Yasunari 1990, Webster and Yang 1992). Although these statistical results may not necessarily clarify the cause-and-effect relationship between the ISM and ENSO, they have led to the implication that the ISM could influence the ongoing ENSO evolutions (Yasunari and Seki 1992, Kirtman and Shukla 2000). Several studies have further found that the El Niño (La Niña) events with a weak ISM in their developing summer, tend to peak with a larger (smaller) amplitude in the following winter than those with the normal monsoon, and vice versa for a strong ISM (Wu and Kirtman 2003, Lin et al 2023). Furthermore, numerical experiments with simple or intermediate coupled models have also claimed that ISM variability can influence the intensity or other statistical properties of ENSO (Nigam 1994, Wainer and Webster 1996, Meehl 1997, Chung and Nigam 1999). Kirtman and Shukla (2000) found that the lag correlation between ISM and ENSO was also reproduced in the intermediate coupled model, even if the parameterized monsoon anomaly was shifted to be centered on December-March. They thus claimed that the lag correlation was mainly determined by the time it took for the Pacific coupled system to respond to the monsoon-induced wind anomalies, rather than by the ENSO phase locking with the annual cycle. The latest study by Lin et al (2023) further revealed the detailed physical processes involved in the effect of the ISM on subsequent ENSO evolution. A weak (strong) monsoon can induce an anomalous cyclonic (anticyclonic) circulation over the western North Pacific (WNP). The westerly (easterly) wind anomalies on the southern flank of the anomalous circulation can affect the following ENSO evolution by exciting Pacific air-sea coupling processes thereafter, and these air-sea interactive processes induced by anomalous ISM were confirmed by a series of sensitivity experiments with a fully coupled climate model.

The latest generation of climate models, participating in the phase 6 of the Coupled Model Intercomparison Project (CMIP6), has recently been released (Eyring et al 2019). While the majority of CMIP6 models exhibit notable improvements in representing the climatological and interannual variability of the ISM compared to the previous generations (Rajendran et al 2022), their performance in simulating the simultaneous correlation between ENSO and ISM in the historical period of 1900–2014 has been improved slightly (Choudhury et al 2022). The CMIP6 models also display a large inter-model spread in the strength of simultaneous correlations between ENSO and ISM (Meehl et al 2023, Yu et al 2023), as observed in the previous generation (Ramu et al 2018). However, as an important aspect of the interaction between monsoons and ENSO, the abilities of CMIP6 models in representing the impacts of ISM

on ENSO and the potential reasons for the intermodel diversity in this regard have not been addressed appropriately. In this study, we assess the performances of 52 CMIP6 models in simulating the ISM's influences on subsequent ENSO evolution and investigate the possible sources of the inter-model spread in the impacts.

2. Data and methods

Observational data used in this study include 1) the monthly SST data from the Hadley Centre Sea Ice and Sea Surface Temperature (HadISST) version 1 (Rayner et al 2003) from 1871 to 2016; 2) the All-India rainfall from the Indian Institute of Tropical Meteorology for the period 1871-2016 (Parthasarathy et al 1994). To examine the intermodel diversity in ISM's impact on ENSO, we analyze the monthly mean outputs of the first realization from the historical simulations of 52 CMIP6 models (table S1 in supplementary material). The monthly mean outputs of the ensemble members 1–50 of the Community Earth System Model Version 2 Large Ensemble (CESM2-LE; Rodgers et al 2021) are also used. All model outputs are horizontally interpolated onto a common $2.5^{\circ} \times 2.5^{\circ}$ grid before analysis.

To ensure the sufficient samples for both anomalous monsoon and ENSO events, the longest time period in the observations is analyzed (1871–2016), and the entire period of historical simulations (i.e. 1850–2014) is considered for CMIP6 models. We have also repeated our analyses using the time period mutually covered by both observations and models (i.e. 1871–2014) and found that the conclusions remained unchanged. Anomaly fields are obtained by calculating their deviations from the climatological seasonal cycle. To focus on the ISM's impacts on ENSO on the interannual timescale, the linear trend of anomaly fields is removed and a 4–108-month bandpass filter is applied to these fields (Park and Burrus 1987).

ENSO variability is represented by the averaged SSTAs in the Niño-3.4 region (170°-120° W, 5° S-5° N). The JJAS rainfall averaged over the Indian region (70°-90° E, 10° -30° N) is used to denote the ISMR variability in the CMIP6 models. Since the ISM variability is not independent from ENSO, that is, a high tendency of El Niño (La Niña) events to co-occur with weak (strong) ISMs, composite anomalies of anomalous ISM years thus also include the influence of ENSO, making it difficult to isolate the anomalies induced by the ISM alone. To better illustrate the ISM's impacts on ENSO, we make a conditional classification as in previous studies (Wu and Kirtman 2003, Lin et al 2023). Specifically, a year of El Niño, La Niña, and non-ENSO is identified when the JJAS-averaged Niño-3.4 SST index is above 0.43, below -0.43, and in the range of -0.43 to 0.43 of its standard deviation (STD), respectively. Similarly, a strong (weak) ISM year is determined by the ISMR index versus its STD. The 0.43 STD is used as the criterion to ensure that the three categories have nearly equal numbers of years, considering an approximately normal distribution with a zero mean for both the Niño-3.4 SST index and the ISMR index. Based on this classification, the El Niño or La Niña events are categorized into three groups: those that co-occur with strong, weak, and normal ISMs (see table S2), referred to as EN (LN)-Wet years, EN (LN)-Dry years, and EN (LN)-Nor years, respectively. The anomalous monsoon years that are independent from ENSO are also identified, referred to as NE-Dry and NE-Wet years. The difference between the ENSO events with and without anomalous ISMs implies the influence of ISM on ENSO. The composite anomaly of NE-Dry and NE-Wet years indicates the impact of anomalous ISM under the ENSO neutral condition. The above classification is also conducted using the December-February (DJF) averaged Niño-3.4 SST index, and the main conclusions remain unchanged.

3. Results

3.1. Diverse impacts of ISM on ENSO in CMIP6 CGCMs

Figure 1(a) exhibits the lead-lag correlations between ISMR and monthly Niño-3.4 SST index. In observations, the maximum negative correlation appears in October-November after the monsoon season. This timing in the ENSO-ISM association implies the potential influences of ISM on the following ENSO evolution, as proposed in previous studies (Webster and Yang 1992, Kirtman and Shukla 2000). To examine the performances of the 52 CMIP6 models in representing the ENSO-ISM relationship, we calculate the correlations between ISMR and Niño-3.4 SST index averaged in the subsequent October-December (OND) in the models and observations (figure 1(b)). There exists a large spread in the correlations among the models. Some models show much weaker values of the correlations compared with observations, while others simulate comparable correlation values. This result may indicate a considerable diversity in the ISM's effects on ENSO among the CMIP6 models. To better depict the diversity, we further divide the 52 models into two groups according to whether or not the lag correlation in the individual models is stronger than the multimodal ensemble (MME) mean of the 52 models, referred to as high-impact models (HIMs) and low-impact models (LIMs), respectively. The MME mean of HIMs effectively reproduces the observed evolution and magnitude of lag correlations during the monsoon season and in the following months (figure 1(a)). By contrast, the MME mean of LIMs simulates relatively weaker values (-0.29)compared to those in both observations (-0.58) and HIMs (-0.51) (figure 1(b)).

One possible scenario that should be discussed here is that the spread observed from the single realizations of CMIP6 models may be determined by internal variability rather than model differences. For example, Bódai et al (2023) claimed that the assessment of model performance with regard to decadal variability of ENSO-ISM teleconnection using a single realization of different CMIP models could lead to spurious model classification. To further examine whether the inter-model spread is governed by internal variability, we repeat the analysis in figure 1(b) by using 50 ensemble members of CESM2-LE. Figure S1 shows that the spread in the lag correlation among the 50 ensemble members is rather small compared to the diversity of the 52 CMIP6 models. The standard deviation of lag correlations across the 50 CESM2-LE ensemble members is 0.05, which is also significantly smaller than that of the CMIP6 models (0.32). These results suggest that the model difference, rather than internal variability, plays a dominant role in the inter-model spread in the lag correlation among single realizations of the 52 CMIP6 model.

To further illustrate the ISM's impacts on ENSO among the CMIP6 models, figure 2 depicts the time evolution of composite Niño-3.4 SSTAs associated with categorized ENSO and anomalous monsoon years. In observations, the El Niño events concurrent with a weak ISM grow more rapidly during the developing summer and autumn, peaking with a larger amplitude in the mature winter compared to the EN-Nor years (figure 2(a)). Conversely, El Niño events co-occurring with a strong monsoon are weaker than those with normal monsoon. Similarly, the La Niña events concurrent with strong monsoon are more intense than those with normal monsoon, and vice versa (figure 2(b)). Anomalous ISMs alone can also affect the central-eastern Pacific SSTs under an ENSO-neutral condition, with notably warm (cold) SSTAs appearing in the subsequent winter after a weak (strong) ISM (figure 2(c)). These composite results can be reproduced successfully by a series of sensitivity experiments based on a fully coupled climate model (NACR CESM1), in which monsoon heating or cooling is imposed in the ENSO developing summer (Lin et al 2023), suggesting that a weak ISM can enhance an ongoing El Niño event but weaken a La Niña event, and conversely for a strong ISM. HIMs reasonably simulate the observed ISM's impacts on Niño3.4 SSTAs during ENSO and non-ENSO years, though some quantitative discrepancies exist (figures 2(d)–(f)). In contrast, LIMs show much smaller differences in Niño3.4 SSTAs between ENSO events concurrent with anomalous ISM and those with normal ISM, indicating a significant underestimation of the ISM's effects on ENSO in these models (figures 2(g) and (h)). Moreover, the Niño3.4 SSTAs during anomalous ISM years without ENSO are also notably weaker in LIMs (figure 2(i)). In summary,

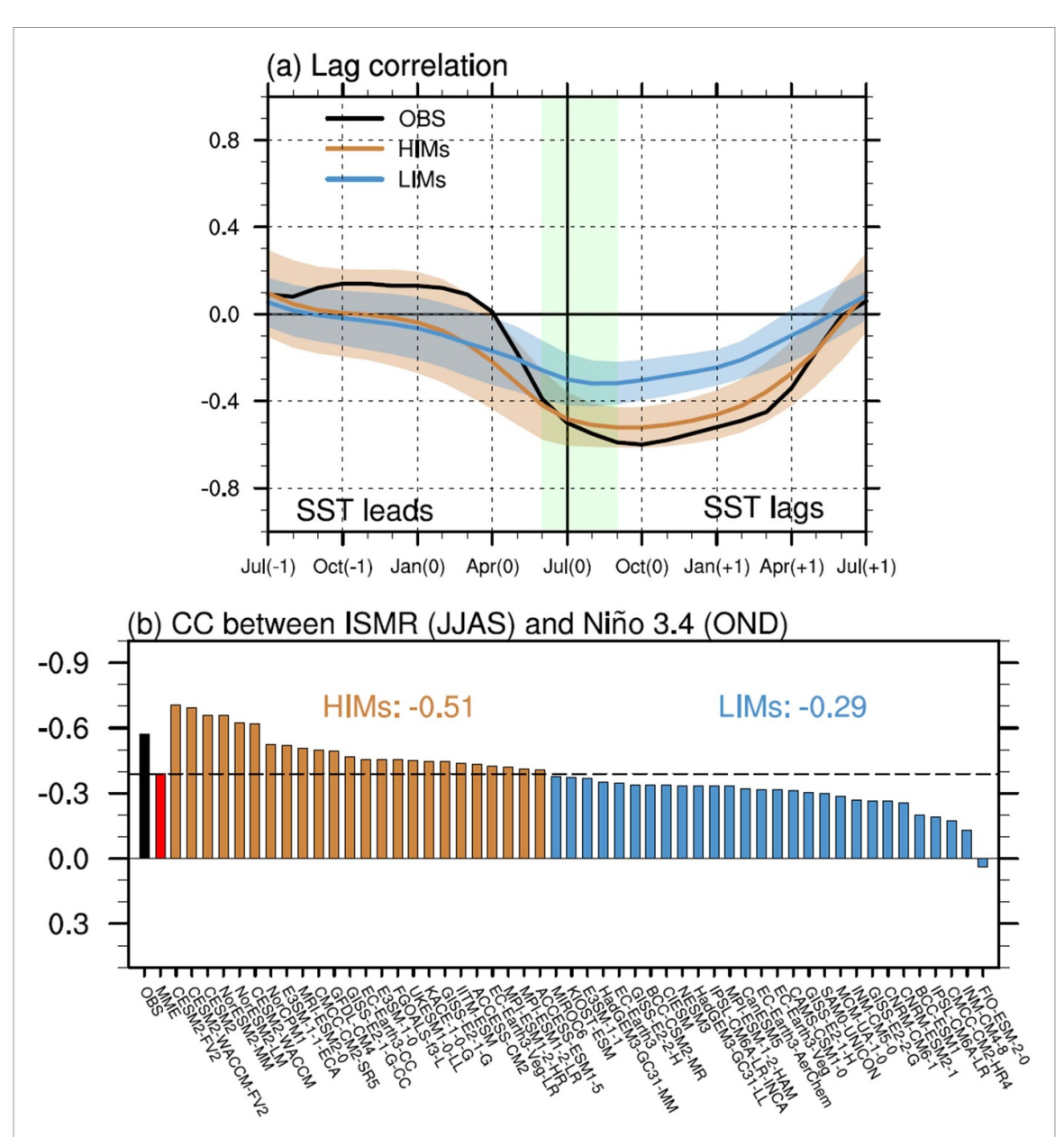


Figure 1. (a) Lead-Lag correlations between ISMR and monthly mean Niño-3.4 SST index. The black line denotes observation, and orange and blue lines represent the MME mean of the models with higher and lower negative correlation coefficients between JJAS ISMR and the Niño-3.4 index in subsequent October–December (OND), referred to as high- and low-impact models (HIMs and LIMs), respectively. Orange and blue shadings indicate the corresponding standard deviations. Green shading highlights the monsoon season. (b) Correlation coefficients between JJAS ISMR and the subsequent OND Niño-3.4 index in observation and 52 CMIP6 models. The black bar indicates observation and the red bar denotes the MME mean of 52 CMIP6 models. Orange (blue) bars highlight the HIMs (LIMs), and the orange (blue) text shows the mean correlations in HIMs (LIMs).

these composite results are consistent with the findings in figure 1 and confirm the substantial differences between HIMs and LIMs in simulating the impacts of ISM on ENSO.

3.2. Causes of model diversity in ISM's influence on ENSO

Figure 3 shows the differences in composite anomalies of precipitation, 850-hPa winds and SST between the EN-Dry and EN-Nor years in HIMs and LIMs. One important feature is that differences in both precipitation and circulation between HIMs and LIMs are large during and after the monsoon season but relatively weak before that (figures 3(a)–(c)). For

HIMs, a substantial reduction in summer rainfall covers the Indian region in the EN-Dry years compared to EN-Nor years, accompanied by significant precipitation and cyclonic circulation differences over the WNP (figure 3(d)). Notably, prominent westerly wind differences prevail over the western Pacific. As demonstrated by Lin *et al* (2023), a weak ISM can cause increased precipitation and associated cyclonic circulation over the WNP, and conversely for a strong ISM. Specifically, a weak ISM can stimulate the atmospheric cold Kelvin waves propagating eastward, resulting in cyclonic wind shear in the lower troposphere of the WNP. The anomalous boundary layer convergence induced by anomalous

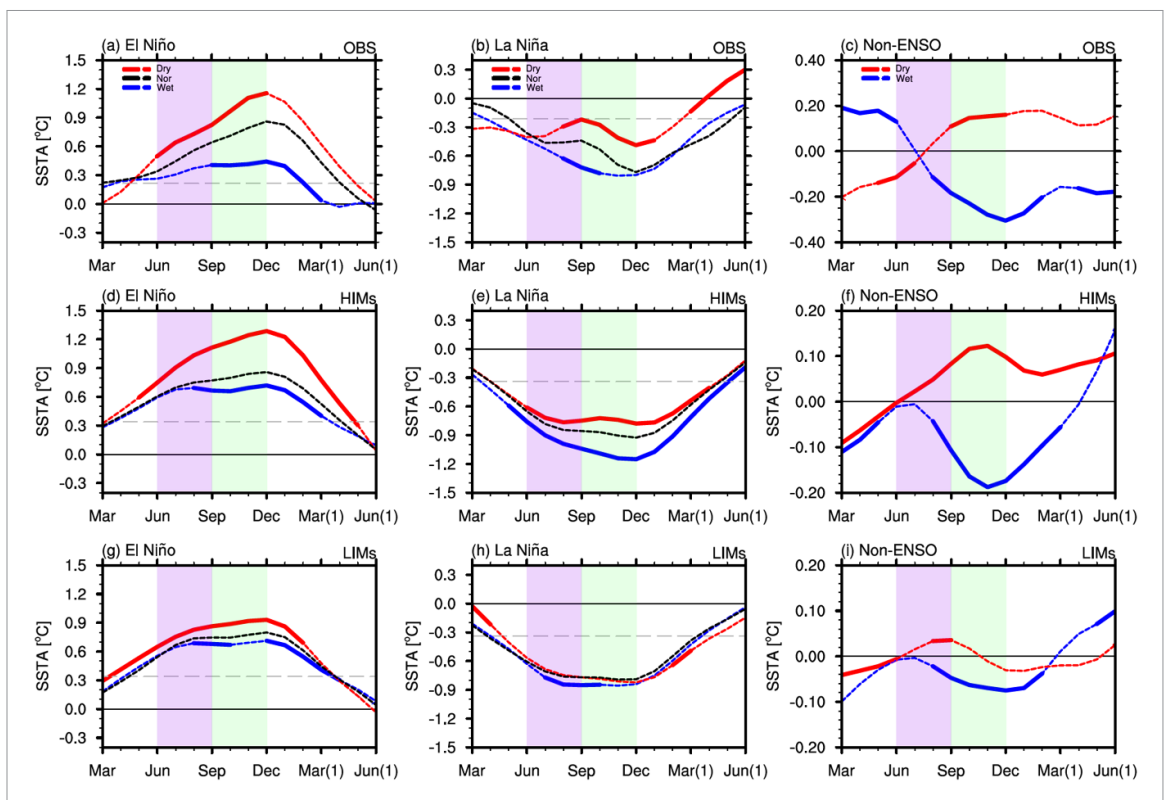


Figure 2. Time series of composite Niño-3.4 SSTAs (units: $^{\circ}$ C) for (a) El Niño, (b) La Niña, and (c) Non-ENSO years with a weak (dry; red line), strong (wet; blue line), or normal ISM (black line) co-occurring during the developing summer. Both (d)–(f) and (g)–(i) are the same as (a)–(c), but for the MME mean of HIMs and LIMs, respectively. Gray dashed lines represent the 0.43 standard deviations of the JJAS-averaged Niño-3.4 index. In (a) and (b), thick curves indicate that the differences in SSTA between ENSO years concurrent with anomalous ISM and those with normal ISM are significant at the 95% confidence level based on the bootstrapping method of Lin *et al* (2023). In (d), (e), (g) and (h), they represent that at least two-thirds model agree on the sign of the MME mean of differences in the SSTA. For (c), (f) and (i), thick curves denote the anomalies at above 95% confidence level and at least two-thirds model agreement on the sign of the MME mean of SSTAs, respectively. Purple and green shadings highlight the monsoon season and the following October–December, respectively.

wind shear increases the WNP precipitation, which in turn induces the anomalous cyclonic circulation as an atmospheric Rossby wave response. The westerly wind anomalies on the southern flank of the circulation can perturb the SSTs in the central-eastern Pacific by inducing oceanic downwelling Kelvin waves and zonal advection of warm water (figure 3(m)). Due to the existence of strong air-sea coupling in the equatorial Pacific during boreal summer and autumn (Tziperman et al 1997, Galanti et al 2002), the positive SST differences are further intensified through exciting the Bjerknes feedback thereafter (Bjerknes 1969) (figure 3(p)). However, the ISMR anomalies are significantly weaker in LIMs compared with HIMs (figures 3(d)–(f)). Accordingly, the ISM-related precipitation and circulation anomalies over WNP are much weaker in LIMs, corresponding to smaller westerly wind anomalies in the western Pacific. The SST differences in the central-eastern Pacific during the subsequent winter, therefore, show smaller values in LIMs in comparison with those in HIMs (figures 3(p)-(r)).

For the EN-Wet years, the precipitation and circulation anomalies show insignificant differences in comparison with EN-Nor years in both HIMs and LIMs before the summer monsoon (figures 4(a) and

(b)). In the monsoon season, HIMs simulate positive precipitation anomalies over the Indian region, while significantly negative values are observed over the WNP (figure 4(d)). A prominent anticyclonic circulation dominates the WNP, with anomalous easterly winds prevailing on its southern flank. The negative SSTAs thus occur in the central-eastern Pacific after the monsoon season (figure 4(p)). Similar to EN-Dry years, the ISMR anomalies are weaker in EN-Wet years in LIMs, accompanied by weaker WNP precipitation and circulation anomalies induced by ISM (figures 4(e) and (f)). Consequently, the differences in El Niño SSTAs are insignificant and smaller in LIMs than those in HIMs in the following months (figures 4(q) and (r)). LIMs also display weaker ISMR anomalies in both LN-Wet and LN-Dry years, corresponding to the weaker precipitation and circulation anomalies over the WNP during the monsoon season (figures S2(d)–(f) and S3(d)–(f)). Therefore, anomalous ISMs also exert weaker impacts on La Niña events in LIMs than HIMs (figures S2(r) and S3(r)). For both NE-Wet and NE-Dry years, the summertime dipole-like rainfall anomalies between the Indian and WNP regions are also pronounced in HIMs but relatively weak in LIMs (figures S4(d)-(f) and S5(d)-(f)). Consistently, there are noticeable SSTAs in the

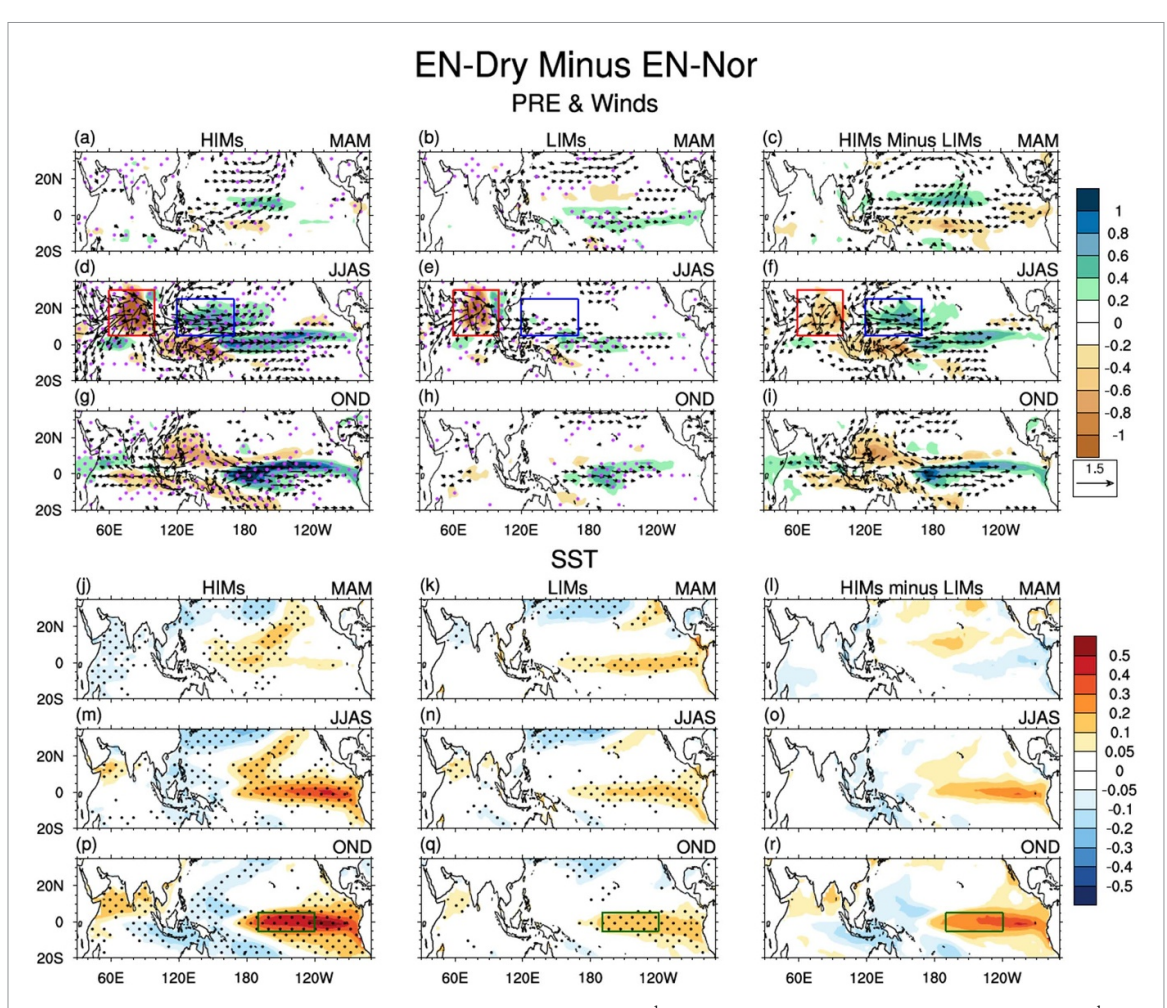
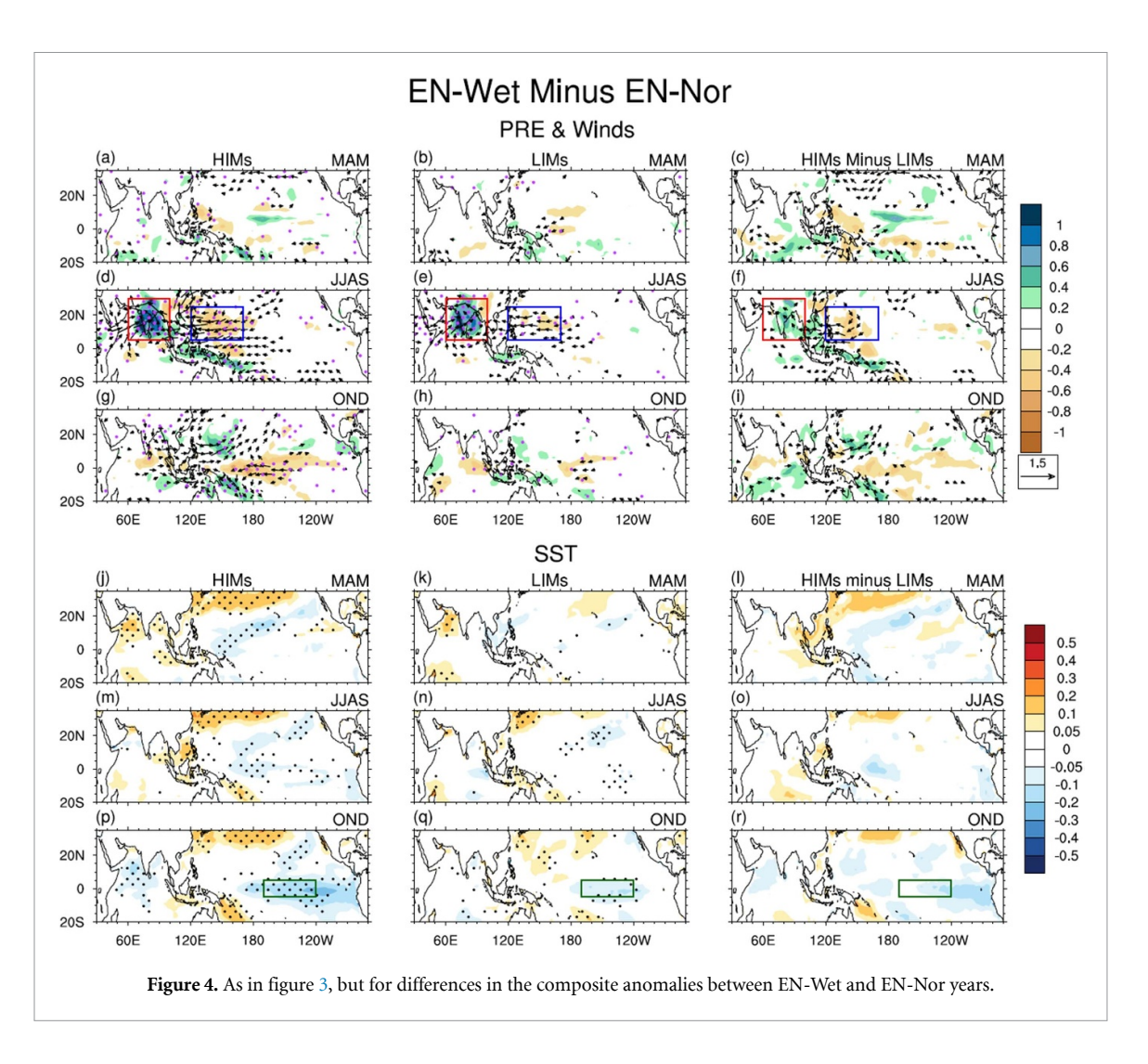


Figure 3. Differences in composite precipitation (shading; units: mm d^{-1}) and 850-hPa wind anomalies (vector; units: ms $^{-1}$) between EN-Dry and EN-Nor years during March–May (MAM) for the MME mean of (a) HIMs, (b) LIMs. (c) Same as (a) and (b), but for the difference between HIMs and LIMs (HIMs minus LIMs). Both (d)–(f) and (g)–(i) are the same as (a)–(c), but for June–September (JJAS) and October–December (OND), respectively. (j)–(r) Same as (a)–(i), but for the differences in composite SSTAs (shading; units: $^{\circ}$ C). Stippling denotes at least two-thirds model agreement on the sign of MME mean. In the left two panels, only the wind vectors with at least two-thirds model agreement on the sign of MME mean are plotted. Red, blue, and green boxes indicate the Indian, WNP, and Niño-3.4 regions, respectively.

central-eastern Pacific after the monsoon season in HIMs, whereas LIMs show comparatively weaker SSTAs (figures S4(p)-(r) and S5(p)-(r)). Indeed, the ISMR anomalies exhibit significantly negative intermodel correlations with those in ISM-induced Niño-3.4 SSTAs during OND in both El Niño and La Niña events (figures S6(a)–(d)). Models with larger negative ISMR anomalies would represent a stronger positive (negative) impact on the El Niño (La Niña) SSTAs, and conversely for a strong ISM. Therefore, the diverse impacts of ISM on ENSO are highly associated with the diverse intensity of ISMR anomalies among the CMIP6 models. Furthermore, there also exist negative inter-model correlations between the ISMR anomalies and OND Niño 3.4 SSTAs in both NE-Dry and NE-Wet years (figures S6(e) and (f)), indicating that the diversity in ISM's effects on Pacific SSTs under ENSO-neutral conditions is also related to the inter-model spread in ISMR anomalies without ENSO.

The inter-model correlation between the interannual variability of ISMR and lag correlation of ISMR and OND Niño-3.4 SST index shows a significant negative value (-0.70; above 95% confidence level), reconfirming that the diverse ISM's impacts on ENSO are closely linked to the inter-model spread in ISMR variability among the models (figure 5(a)). The ISMR variability in HIMs is about 32% larger than that in LIMs. Given that the intensity of ISM's impact on ENSO also relies on the strength of air-sea coupling in the Pacific Ocean, we calculate the Bjerknes feedback intensity (BFI) in the CMIP6 models to examine whether the inter-model spread in the strength of Pacific air-sea coupling could potentially influence the diversity of the ISM's impacts on ENSO. Detailed descriptions of the BFI can be seen in Text S1 in supplementary material. The BFI is negatively correlated with the lag correlation between ISMR variability and OND Niño-3.4 SST index among the CMIP6 models, suggesting that



models with a stronger BFI tend to simulate a larger impact of ISM on ENSO (figure 5(b)). However, the inter-model correlation coefficient is statistically insignificant and small, and the difference in BFI between HIMs and LIMs is also negligible. Therefore, the main cause of the diverse influences of ISM on ENSO is the diversity in ISMR variability, rather than that in the air-sea coupling strength in the tropical Pacific.

4. Discussion

We find that the difference in ISM's impacts on ENSO is primarily attributed to the difference in ISMR variability between HIMs and LIMs. The potential processes for the differences in ISMR variability are discussed below. In EN-Dry and LN-Wet years, the monsoon anomalies are related to the concurrent ENSO, and the ENSO-monsoon interaction is strong (Webster and Yang 1992, Kirtman and Shukla 2000, Lin *et al* 2023). HIMs exhibit larger ISMR anomalies during EN-Dry and LN-Wet years compared to LIMs, possibly due to a stronger ENSO amplitude during the monsoon season in HIMs. In the summer of EN-Dry years, the El Niño SSTAs are warmer

in HIMs than in LIMs (figures 3(m)-(o)), which can cause a substantial monsoon precipitation deficit by inducing a strong anomalous Walker circulation, consistent with the higher simultaneous correlations between ENSO and ISM (figure 1(a)). Recent studies have also shown that the CMIP6 models with larger ENSO amplitude tend to simulate a stronger simultaneous ENSO-ISM relationship (Meehl et al 2023, Yu et al 2023). The larger ISMR anomalies, in turn, exert stronger feedback on ENSO. The warmer summertime SSTAs and resultant stronger ENSOmonsoon interaction in HIMs may be attributed to the pronounced westerly wind anomalies over the western Pacific in the preceding spring (figure 3(a)), which are associated with the springtime SSTAs in the subtropical central Pacific (figure 3(j)). The wind anomalies may trigger oceanic downwelling Kelvin waves that transport subsurface warm water eastward, thereby facilitating the El Niño development from the spring to summer. By contrast, in LIMs the subtropical warm SSTAs are weak (figure 3(k)), and the wind anomalies are not present in the western Pacific but are confined to the central-eastern Pacific (figure 3(b)). Similar results are observed in LN-Wet years (figures S2(a)-(c) and (j)-(l)). Indeed, there are

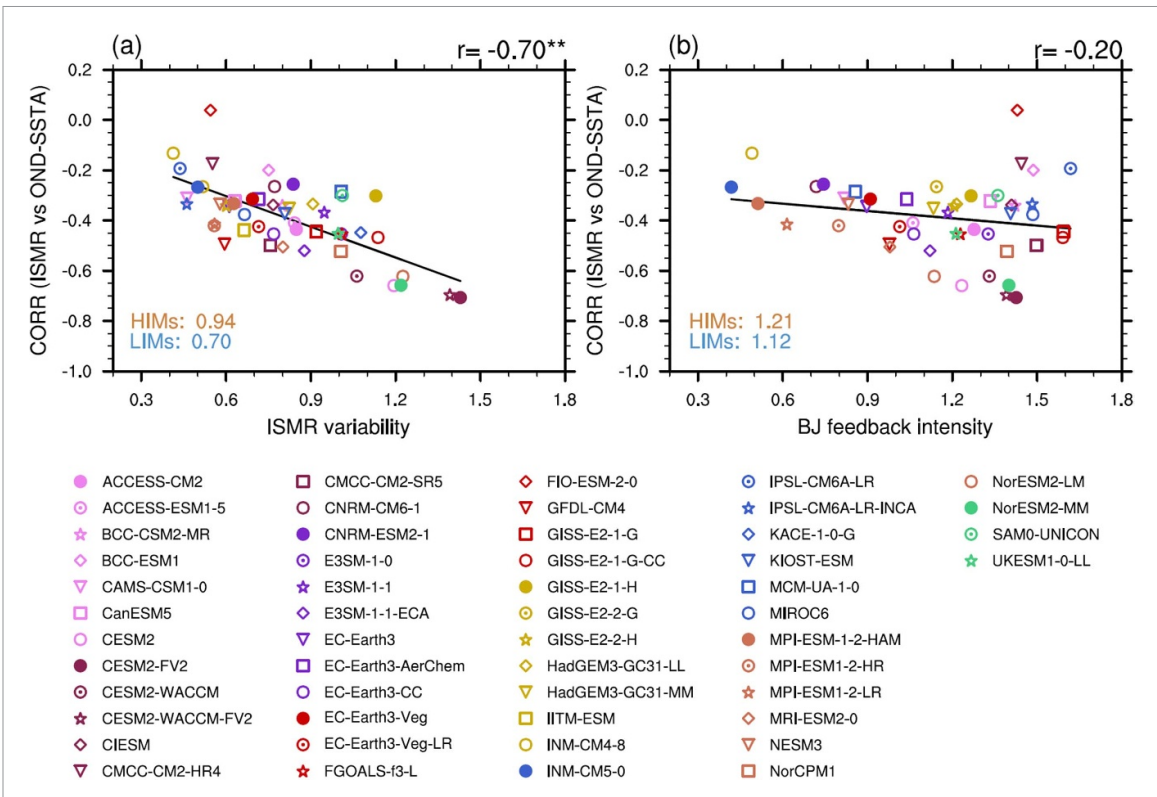


Figure 5. (a) Scatterplots of ISMR variability and lag correlation between ISMR and OND Niño-3.4 SST index among 52 CMIP6 models. (b) Same as (a), but for Bjerknes feedback intensity and lag correlation. Black lines denote the linear fit, and the correlation coefficient is shown in the top-right corner. The significant correlation coefficients at the 95% level based on the two-sided Student's *t*-test are indicated by two asterisks.

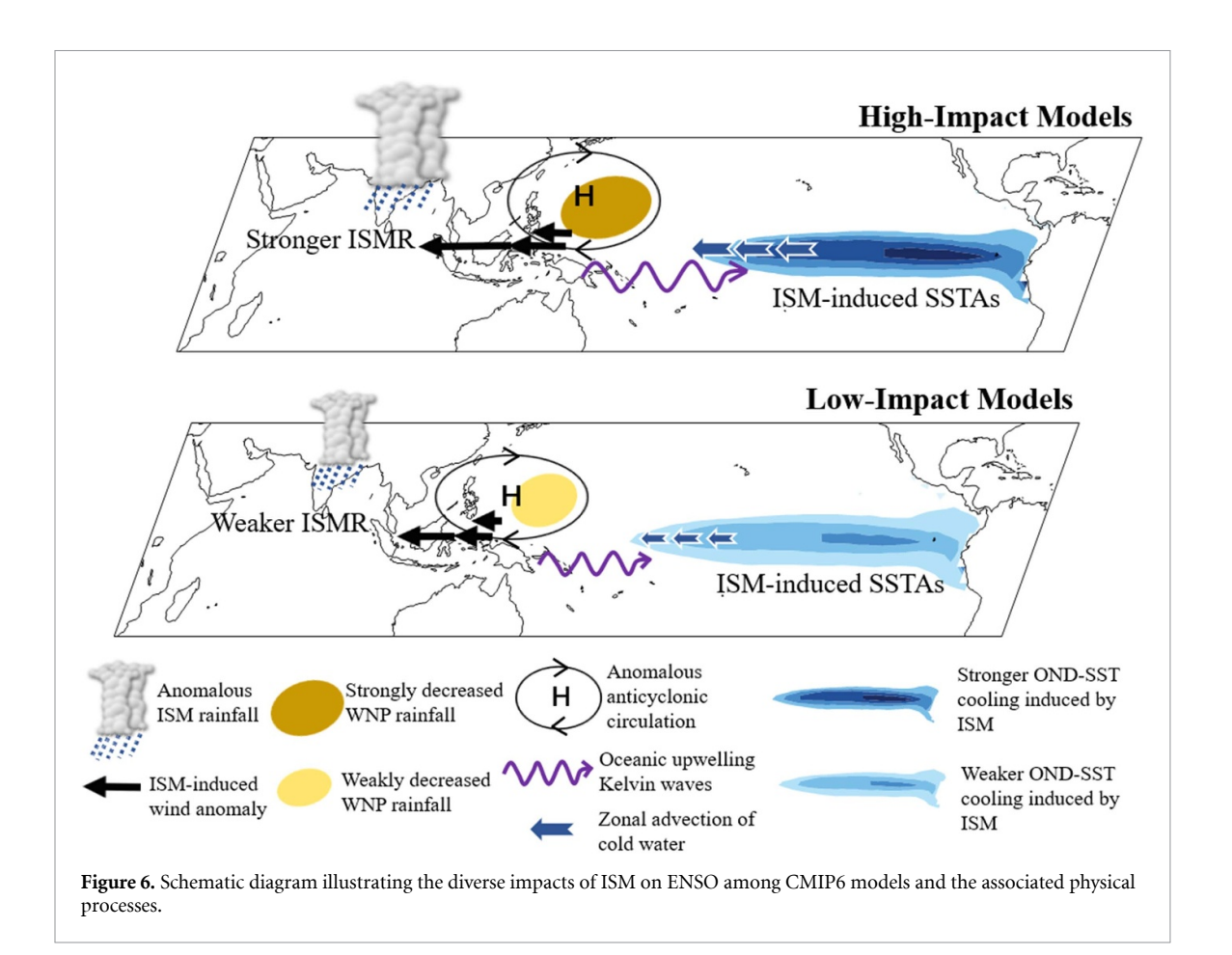
significant differences in the amplitude of SSTAs in the central-eastern Pacific between HIMs and LIMs (figure S7(a)). Moreover, the inter-model correlation between ISMR variability and ENSO amplitude during JJAS is 0.56, explaining about 31% inter-model variation of interannual variability of ISMR (figure S7(b)).

During the EN-Wet (LN-Dry) years, the concurrent El Niño (La Niña) SSTAs are less likely to cause the strong (weak) ISM. Apart from the ENSO effects, the interannual variability of ISM is also influenced by other boundary forcings, including SSTs in the Indian Ocean (Ashok et al 2001, Crétat et al 2017) and Atlantic Ocean (Kucharski et al 2008, Sabeerali et al 2019), as well as surface air temperature over the Eurasian continent related to land surface conditions (e.g. snow cover and soil moisture) (Parthasarathy and Yang 1995, Yang and Lau 1998, Robock et al 2003, Halder and Dirmeyer 2017). Atmospheric internal dynamics also account for a large portion of the ISM variability (Goswami 1998, Hsu and Yang 2016). However, insignificant differences in summertime SSTAs between HIMs and LIMs are observed in the tropical Indian Ocean (figures 4(o) and S3(o)) and Atlantic Ocean (figure not shown) in EN-Wet and LN-Dry years, as well as in both NE-Wet (figure S4(o)) and NE-Dry years (figure S5(o)). Consistently, the differences in

SSTA amplitude between HIMs and LIMs are negligible in the two oceans (figure S7(a)). Additionally, there are no significant surface air temperature anomalies over the Eurasian continent (figure S8) that could explain the differences in monsoon anomalies between the two groups of models. The difference in ENSO-unrelated ISMR anomalies between the two groups of models might be associated with atmospheric internal dynamics or other potential factors, requiring further investigation in future studies.

5. Conclusions

In this study, we examine the performances of 52 CMIP6 models in representing the influences of ISM on the following ENSO evolution. The results reveal a significant inter-model diversity in the impacts of ISM on ENSO. Although some models can simulate the impacts comparable to observations, others represent notably weaker influences. The primary factors contributing to the diverse impacts are investigated and summarized in figure 6. The diversity in ISM's effects on ENSO is highly associated with the simulated amplitude of ISMR interannual variability. Models with a larger ISMR variability simulate a higher ISM's impacts on ENSO,



while those with a smaller ISMR variability simulate weaker influences of ISM on ENSO. The strongly increased ISMR can cause more pronounced negative precipitation anomaly and anticyclonic circulation over the WNP. The larger easterly wind anomalies over the western Pacific induced by the ISM can lead to cold SSTAs in the central-eastern Pacific in the following seasons by exciting stronger oceanic upwelling Kelvin waves and zonal advection of cold water. The inter-model diversity in the ENSO-related monsoon amplitude among the models may be linked to the ENSO amplitude during the boreal summer. Models with a larger ENSO amplitude would simulate a larger ISMR anomaly and stronger ENSO-ISM interaction, and vice versa. The differences in the ENSO-unrelated monsoon variability between strong and weak-impact models remain unclear and further studies are needed. Our findings could contribute to enhancing the skills of climate models in capturing the ENSO-monsoon interactions.

Data availability statement

The HadISST1 dataset is downloaded from the UK Met Office (www.metoffice.gov.uk/hadobs/hadisst/).

The all-India monthly rainfall dataset is provided by the Indian Institute of Tropical Meteorology at https://tropmet.res.in/data/data-archival/rain/iitm-regionrf.txt. The monthly outputs of CMIP6 models used in this study are available at the Earth System Grid Federation (https://esgf-index1.ceda.ac.uk/search/cmip6-ceda/). The monthly outputs of CESM2-LE are available at www.earthsystemgrid.org/dataset/ucar.cgd.cesm2le.output.html.

All data that support the findings of this study are included within the article (and any supplementary files).

Acknowledgments

The authors thank Dr Shan He from Stony Brook University, State University of New York, and the three anonymous reviewers for their constructive comments and suggestions on the early version of this paper. This study was jointly supported by the National Key Research and Development Program of China (Grant 2020YFA0608803), the National Natural Science Foundation of China (Grants 42175023), the Innovation Group Project of Southern Marine Science and Engineering Guangdong Laboratory (Zhuhai) (Grant 311021001),

the Guangdong Province Key Laboratory for Climate Change and Natural Disaster Studies (Grant 2020B1212060025), and the China Scholarship Council Joint PhD Training Program. The authors declare no competing financial interests.

ORCID iDs

Shuheng Lin https://orcid.org/0000-0001-8951-7417

Buwen Dong 6 https://orcid.org/0000-0003-0809-

Song Yang https://orcid.org/0000-0003-1840-8429 Tuantuan Zhang https://orcid.org/0000-0002-1635-0625

References

- Ashok K, Guan Z and Yamagata T 2001 Impact of the Indian Ocean dipole on the relationship between the Indian monsoon rainfall and ENSO *Geophys. Res. Lett.* **28** 4499–502
- Bjerknes J 1969 Atmospheric teleconnections from the equatorial Pacific *Mon. Weather Rev.* **97** 163–72
- Bódai T, Aneesh S, Lee J Y and Lee S S 2023 Decadal Indian Ocean influence on the ENSO-Indian monsoon teleconnection mostly apparent *J. Geophys. Res. Atmos.* **128** e2023JD038673
- Choudhury B A, Rajesh P V, Zahan Y and Goswami B N 2022 Evolution of the Indian summer monsoon rainfall simulations from CMIP3 to CMIP6 models *Clim. Dyn.* 58 2637–62
- Chowdary J, Xie S P and Nanjundiah R S 2021 Drivers of the Indian summer monsoon climate variability *Indian Summer Monsoon Variability* (Elsevier) ch 1, pp 1–27
- Chung C and Nigam S 1999 Asian summer monsoon-ENSO feedback on the Cane-Zebiak model ENSO *J. Clim.* 12 2787–807
- Crétat J, Terray P, Masson S, Sooraj K P and Roxy M K 2017 Indian Ocean and Indian summer monsoon: relationships without ENSO in ocean–atmosphere coupled simulations Clim. Dyn. 49 1429–48
- Eyring V *et al* 2019 Taking climate model evaluation to the next level *Nat. Clim. Change* 9 102–10
- Gadgil S and Gadgil S 2006 The Indian monsoon, GDP and agriculture *Econ. Political Wkly.* **41** 4887–95 (available at: www.jstor.org/stable/4418949)
- Galanti E, Tziperman E, Harrison M, Rosati A, Giering R and Sirkes Z 2002 The equatorial thermocline outcropping-A seasonal control on the tropical Pacific ocean-atmosphere instability strength J. Clim. 15 2721–39
- Goswami B N 1998 Interannual variations of Indian summer monsoon in a GCM: external conditions versus internal feedbacks *J. Clim.* 11 501–22
- Halder S and Dirmeyer P A 2017 Relation of Eurasian snow cover and Indian summer monsoon rainfall: importance of the delayed hydrological effect *J. Clim.* 30 1273–89
- Hsu P C and Yang Y 2016 Contribution of atmospheric internal processes to the interannual variability of the South Asian summer monsoon *Int. J. Climatol.* **36** 2917–30
- Ju J and Slingo J 1995 The Asian summer monsoon and ENSO Q. J. R. Meteorol. Soc. 121 1133–68
- Kirtman B P and Shukla J 2000 Influence of the Indian summer monsoon on ENSO Q. J. R. Meteorol. Soc. 126 213–39
- Kucharski F, Bracco A, Yoo J H and Molteni F 2008 Atlantic forced component of the Indian monsoon interannual variability Geophys. Res. Lett. 35 1–5
- Kumar K K, Rajagopalan B and Cane M A 1999 On the weakening relationship between the Indian monsoon and ENSO Science 284 2156–9

- Kumar K K, Rajagopalan B, Hoerling M, Bates G and Cane M 2006 Unraveling the mystery of Indian monsoon failure during El Niño *Science* 314 115–9
- Lau K M and Yang S 1996 The Asian monsoon and predictability of the tropical ocean-atmosphere system Q. J. R. Meteorol. Soc. 122 945–57
- Lin S, Yang S, He S, Fan H, Chen J, Dong W, Wu J and Guan Y 2023 Atmospheric–oceanic processes over the Pacific involved in the effects of the Indian summer monsoon on ENSO *J. Clim.* **36** 6021–43
- Meehl G A 1997 The south Asian monsoon and the tropospheric biennial oscillation *I. Clim.* 10 1921–43
- Meehl G A *et al* 2023 Climate base state influences on South Asian monsoon processes derived from analyses of E3SMv2 and CESM2 *Geophys. Res. Lett.* **50** e2023GL104313
- Miyakoda K, Kinter J L and Yang S 2003 The role of ENSO in the South Asian monsoon and pre-monsoon signals over the Tibetan plateau *J. Meteorol. Soc. Japan* 81 1015–39
- Nigam S 1994 On the dynamical basis for the Asian summer monsoon rainfall-El Niño relationship *J. Clim.* 7 1750–71
- Pant G B and Parthasarathy S B 1981 Some aspects of an association between the Southern Oscillation and Indian summer monsoon *Arch. Meteorol. Geophys. Bioklimatol.* B **29** 245–52
- Park T W and Burrus C S 1987 Digital Filter Design (Wiley)
 Parthasarathy B, Munot A A and Kothawale D R 1994 All-India monthly and seasonal rainfall series: 1871–1993 Theor. Appl. Climatol. 49 217–24
- Parthasarathy B and Yang S 1995 Relationships between regional Indian summer monsoon rainfall and Eurasian snow cover *Adv. Atmos. Sci.* 12 143–50
- Rajendran K, Surendran S, Varghese S J and Sathyanath A 2022 Simulation of Indian summer monsoon rainfall, interannual variability and teleconnections: evaluation of CMIP6 models Clim. Dyn. 58 2693–723
- Ramu D A, Chowdary J S, Ramakrishna S S V S and Kumar O S R U B 2018 Diversity in the representation of large-scale circulation associated with ENSO-Indian summer monsoon teleconnections in CMIP5 models *Theor. Appl. Climatol.* 132 465–78
- Rasmusson E M and Carpenter T H 1983 The relationship between eastern equatorial Pacific sea surface temperatures and rainfall over India and Sri Lanka *Mon. Weather Rev.* 111 517–28
- Rayner N A, Parker D E, Horton E B, Folland C K, Alexander L V, Rowell D P, Kent E C and Kaplan A 2003 Global analyses of sea surface temperature, sea ice, and night marine air temperature since the late nineteenth century *J. Geophys. Res. Atmos.* **108** 4407
- Robock A, Mu M, Vinnikov K and Robinson D 2003 Land surface conditions over Eurasia and Indian summer monsoon rainfall *J. Geophys. Res. Atmos.* **108** 4131
- Rodgers K B *et al* 2021 Ubiquity of human-induced changes in climate variability *Earth Syst. Dyn.* **12** 1393–411
- Sabeerali C T, Ajayamohan R S, Bangalath H K and Chen N 2019 Atlantic zonal mode: an emerging source of Indian summer monsoon variability in a warming world *Geophys. Res. Lett.* 46 4460–7
- Taschetto A S, Ummenhofer C C, Stuecker M F, Dommenget D, Ashok K, Rodrigues R R and Yeh S W 2020 ENSO atmospheric teleconnections *El Niño Southern Oscillation in a Changing Climate* (American Geophysical Union (AGU)) ch 14, pp 309–35
- Tziperman E, Zebiak S E and Cane M A 1997 Mechanisms of seasonal—ENSO interaction *J. Atmos. Sci.* **54** 61–71
- Wahl E R and Morrill C 2010 Toward understanding and predicting monsoon patterns *Science* 328 437–8
- Wainer I and Webster P J 1996 Monsoon/El Nino-Southern oscillation relationships in a simple coupled ocean-atmosphere model *J. Geophys. Res.* **101** 25599–614

- Webster P J and Yang S 1992 Monsoon and ENSO: selectively interactive systems Q. J. R. Meteorol. Soc. 118 877–926
- Wu R and Kirtman B P 2003 On the impacts of the Indian summer monsoon on ENSO in a coupled GCM Q. J. R. Meteorol. Soc. 129 3439–68
- Yang S, Deng K and Duan W 2018a Selective interaction between monsoon and ENSO: effects of annual cycle and spring predictability barrier *Chin. J. Atmos. Sci.* 42 570–89
- Yang S and Lau K M 1998 Influences of sea surface temperature and ground wetness on Asian summer monsoon *J. Clim.* 11 3230–46
- Yang S, Li Z, Yu J Y, Hu X, Dong W and He S 2018b El Niño-Southern Oscillation and its impact in the changing climate *Natl Sci. Rev.* **5** 840–57
- Yasunari T 1990 Impact of Indian monsoon on the coupled atmosphere/ocean system in the tropical Pacific *Meteorol. Atmos. Phys.* 44 29–41

- Yasunari T and Seki Y 1992 Role of the Asian monsoon on the interannual variability of the global climate system *J. Meteorol. Soc. Japan* **70** 177–89
- Yeh S-W *et al* 2018 ENSO Atmospheric teleconnections and their response to greenhouse gas forcing *Rev. Geophys.* **56** 185–206
- Yu S, Fan L, Zheng X, Zhang Y, Zhou Z and Li Z 2023 Sources of inter-model diversity in the strength of the relationship between the Indian summer monsoon rainfall and El Niño-Southern oscillation *Geophys. Res. Lett.*50 e2022GL101718
- Yuan S, Xu J, Chan J C L, Chiu L S and Pan Y 2020 Resonance effect in interaction between south Asian summer monsoon and ENSO during 1958–2018 J. Trop. Meteorol. 26 137–49
- Zhang R, Sumi A and Kimoto M 1999 A diagnostic study of the impact of El Niño on the precipitation in China *Adv. Atmos. Sci.* **16** 229–41